Analyst

COMMUNICATION

A novel solid-state electrochemiluminescence sensor for the determination of hydrogen peroxide based on an Au nanocluster–silica nanoparticle nanocomposite†

Yanfang Wu,[a] Jinhua Huang,[a] Tingyao Zhou,[a] Mingcong Rong,[a] Yaqi Jiang[a] and Xi Chen*[ab]

A gold nanocluster@bovine serum albumin–silica nanoparticle composite has been synthesized and used for the solid-state electrochemiluminescence (ECL) sensing of hydrogen peroxide. The ECL characteristics have also been studied.

Due to their intriguing physical and chemical properties, metal nanoclusters (MNCs) with sub-nanometer core sized clusters are now being extensively studied for their promising applications in optoelectronics, sensing and catalysis.[1,2] Several metal clusters have been synthesized using various templates such as thiols,[3] polymers,[4] proteins,[5] DNA[6] and peptide.[7] Among these approaches, the usage of a protein as the scaffold for the synthesis holds many advantages such as easy size control, high stability across a wide range of pH, and higher ionic strength. Recently, using a simple and "green" one phase method,[5] a new synthesis approach for fluorescent gold nanoclusters (AuNCs), AuNCs@bovine serum albumin (AuNCs@BSA), is reported, which has been applied in the fields of sensing and bio-imaging because of its ultrafine size, good photo-stability and low toxicity.

Electrogenerated chemiluminescence (ECL), generated from the excited state of an ECL luminophore using electrochemical techniques,[8–13] has been applied to the fields of immunoassay,[14] clinical sensing,[15] and environmental monitoring[16,17] owing to its high sensitivity and extremely wide dynamic range. In recent years, due to the unique physical and chemical properties of nanomaterials (NMs), including nanoparticles (NPs), quantum dots and MNCs,[18–22] great efforts have been made to investigate their applications in ECL. The ECL behaviour of AuNCs, generally in the form of AuNCs@BSA, has been reported for the

detection of H_2O_2, dopamine and Pb^{2+},[23–27] indicating that this could become a promising material for ECL investigation and sensing applications. Unfortunately, these studies are still at an early stage and use solution-phase ECL, with the resulting high consumption of MNCs.

Solid-state ECL, through the immobilization of an ECL luminophore onto an electrode surface, presents several advantages over solution-phase ECL, such as notably enhanced ECL intensity, reduced amount of reagent and simplified experimental design.[12] So far, many immobilization processes such as ion exchange,[28] doping,[29] polymerization,[22] covalent binding[30] and self-assembling methods[31] have been developed for the fabrication of solid-state ECL electrodes with active luminescent materials. Here, we describe the fabrication of a novel solid-state ECL sensor, in which an AuNC@BSA–silica NP nanocomposite was modified onto a glassy carbon electrode (GCE) surface. Its sensing performance for hydrogen peroxide and the effect of the MNCs' dispersion by silica NPs on the solid-state ECL behavior were also investigated.

The AuNC@BSA–silica NP nanocomposite was synthesized using a multistep procedure (shown in Scheme 1). The silica
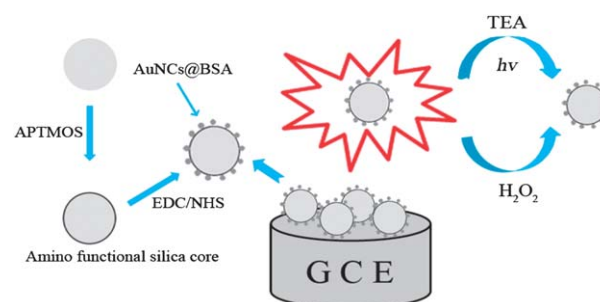
Scheme 1 Schematic representation of the formation of the AuNC@BSA–silica NP nanocomposite and fabrication of the solid-state ECL sensor. The ECL-active luminophore, AuNCs@BSA, was covalently conjugated to the surface of silica NPs functionalized with amino groups. The solid-state ECL sensor was formed by the use of an AuNC@BSA–silica NP nanocomposite and studied for H_2O_2 sensing because H_2O_2 was found to have the ability to destroy this nanocomposite.

[a]Department of Chemistry and Key Laboratory of Analytical Sciences of Xiamen University, College of Chemistry and Chemical Engineering, Xiamen University, Xiamen, 361005, China. E-mail: xichen@xmu.edu.cn; Fax: +86 592 2184530; Tel: +86 592 2184530

[b]State Key Laboratory of Marine Environmental Science, Xiamen University, Xiamen, 361005, China

cores were firstly synthesized, and their surfaces were then modified with amino groups. The following step involved the covalent binding of AuNCs@BSA on the particle surfaces through amino coupling. Silica cores of approximately 250 nm were prepared by a modified Stöber-based synthesis method.[32] The surface modification of the silica cores with amino groups was achieved by direct hydrolysis and co-condensation of (3-aminopropyl)trimethoxysilane with the silica cores in the original ethanol–ammonium hydroxide mixture.[33] The surface-modified silica cores were then dispersed in an aqueous solution of AuNCs@BSA prepared according to the reported method.[5] The AuNCs@BSA was covalently linked to the surface of the silica cores, as a result of the amide bonds formed between the amino groups of the particles and the carboxyl groups from the amino acid residue in the AuNCs@BSA, using EDC/sulfo-NHS chemistry. Finally, the mixture of the AuNC@BSA–silica NP nanocomposite and the Nafion solution was dropped onto the GCE electrode which was then air dried.

The as-prepared silica NPs and the AuNC@BSA–silica NP nanocomposite were characterized as indicated in Fig. 1. The silica NPs were used to covalently link the AuNCs@BSA, effectively distributing it over the large surface area of the particles. The inset in Fig. 1(a) shows the morphology of the silica NPs with a diameter of about 250 nm. After the covalent connection of the AuNCs@BSA onto the surface of the silica NPs, an obvious fluorescence at about 620 nm (excitation at about 370 nm), consistent with that of AuNCs@BSA,[5] could be observed. The distribution of the AuNCs@BSA on the silica NP can be clearly seen from the TEM picture in Fig. 1(c). After being dropped and dried on the GCE, its ECL performance *versus* cyclic potential scanning was conducted as shown in Fig. 1(d). Compared to the solution-phase ECL system reported

previously,[26] similar performance could be seen in that the ECL intensity increased when the potential was scanned over 0.8 V and reached its maximum value of around 1.3–1.4 V (*vs.* Ag/AgCl). The potential step method was used to conduct the ECL experiments. The applied potential obviously affected the whole ECL process including the oxidation of the triethylamine (TEA) and the AuNCs@BSA and thus the generation of the excited state of AuNCs@BSA*. Therefore, the potential-dependent ECL intensity was first investigated to determine optimal performance. As shown in Fig. 2(a), the ECL intensity dramatically increased with the increase of the applied potential and reached a steady state when the applied potential exceeded 1.3 V. On consideration of the stability and the best ECL performance, 1.4 V was chosen for the later ECL experiments.

As is well-known, the detection of hydrogen peroxide (H_2O_2) is of great importance since H_2O_2 plays a significant role in the outgrowth of some substrate-specific enzymatic reactions,[10,34] as well as being an essential intermediate in food, pharmacy, and biological and environmental monitoring. H_2O_2 was found to have the ability to destroy the structure of the AuNCs@BSA and thus disturb its properties,[24,35] hence resulting in the decrease of ECL intensity. Scheme 1 shows the model of the ECL sensing process for H_2O_2 using the AuNC@BSA–silica NP nanocomposite. The anodic ECL originated from the formation of excited-state AuNCs* *via* electron-transfer annihilation. After H_2O_2 was added into the ECL testing system, the anodic ECL intensity displayed an obvious decrease as shown in Fig. 2(c). The decrease was attributed to the excited state of AuNCs* quenched by H_2O_2. The ECL intensity decreased linearly with the increasing concentration of H_2O_2. As shown in Fig. 2(d), the linear range of H_2O_2 concentration and ECL intensity was found
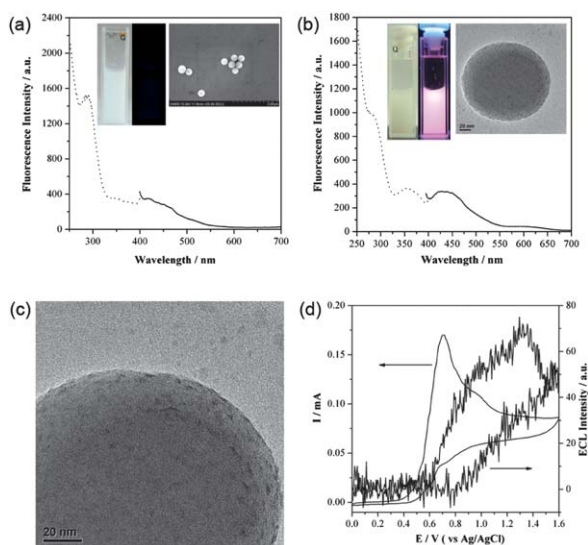
Fig. 1 (a and b) The excitation and emission spectra of silica cores and the AuNC@BSA–silica NP nanocomposite; inset: electron microscope figures and photographs (under UV and ordinary white light, respectively). (c) TEM image of the AuNC@BSA–silica NP nanocomposite and (d) cyclic voltammogram and the corresponding ECL curve of the solid-state ECL sensor in a 0.1 M LiClO$_4$ solution with 70 mM TEA. Scanning rate: 100 mV s^{-1}.
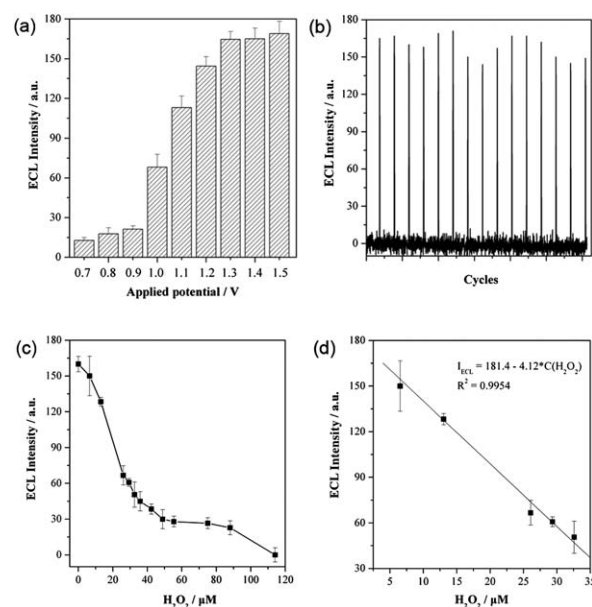
Fig. 2 (a) Histogram displaying the applied potential-dependent ECL intensity of the solid-state ECL sensor; (b) consecutive ECL intensity in 0.1 M LiClO$_4$ with 70 mM TEA; (c) relationship of the response ECL curves *versus* the H_2O_2 concentration and (d) calibration curve between the ECL intensity and the H_2O_2 concentration in 0.1 M LiClO$_4$, 70 mM TEA.

to be 6.5–32.6 μM ($R^2 = 0.9954$). Stable ECL intensities under consecutive potential steps from 0 to 1.4 V for 15 cycles in the ECL testing system are shown in Fig. 2(b). The corresponding signal with an RSD of 7.5% indicated its reasonable stability and reliability for H_2O_2 detection. The H_2O_2 ECL biosensor avoided the use of horseradish peroxidase or hemoglobin, which though normally used in electrochemical detection are of short-term stability. In addition, results (see Fig. S1 in the ESI†) showing the effect of the MNCs' dispersion by silica NPs on solid-state ECL behaviour indicated that silica NPs served as the carrier for the AuNCs@BSA, and could modulate the response of the solid-state ECL sensor toward H_2O_2, resulting in a reasonable behaviour for the determination. Therefore, the model of an ECL biosensor based on the AuNC@BSA–silica NP nanocomposite will provide a new strategy for the detection of H_2O_2.

In conclusion, a novel solid-state ECL sensor for the determination of H_2O_2 based on an AuNC@BSA–silica NP composite was constructed for the first time, and its ECL behaviour as well as preliminary work concerning H_2O_2 sensing were also studied. Results indicated that the ECL system showed acceptable sensitivity for H_2O_2 detection. Since the distribution on silica NPs resulted in a detectable behaviour, further studies on the effect of substrates with different composition and size being used for the construction of MNC-based solid-state ECL sensors will continue. With the advantages of low toxicity, high stability, and easier preparation, we believe that ECLs of MNCs with diverse scaffolds, including AuNCs@BSA, can be promising candidates for ECL analysis.

Notes and references

1 P. L. Xavier, K. Chaudhari, A. Baksi and T. Pradeep, *Nano Rev.*, 2012, **3**, 14767.

2 L. Shang, S. Dong and G. U. Nienhaus, *Nano Today*, 2011, **6**, 401.

3 Y. Negishi, Y. Takasugi, S. Sato, H. Yao, K. Kimura and T. Tsukuda, *J. Am. Chem. Soc.*, 2004, **126**, 6518.

4 H. Duan and S. Nie, *J. Am. Chem. Soc.*, 2007, **129**, 2412.

5 J. Xie, Y. Zheng and J. Y. Ying, *J. Am. Chem. Soc.*, 2009, **131**, 888.

6 J. T. Petty, J. Zheng, N. V. Hud and R. M. Dickson, *J. Am. Chem. Soc.*, 2004, **126**, 5207.

7 J. Yu, S. A. Patel and R. M. Dickson, *Angew. Chem., Int. Ed.*, 2007, **46**, 2028.

8 P. Bertoncello, *Front. Biosci.*, 2011, **16**, 1084.

9 J. Lei and H. Ju, *TrAC, Trends Anal. Chem.*, 2011, **30**, 1351.

10 P. Bertoncello and R. J. Forster, *Biosens. Bioelectron.*, 2009, **24**, 3191.

11 L. Hu and G. Xu, *Chem. Soc. Rev.*, 2010, **39**, 3275.

12 W. Miao, *Chem. Rev.*, 2008, **108**, 2506.

13 M. M. Richter, *Chem. Rev.*, 2004, **104**, 3003.

14 W. Miao and A. J. Bard, *Anal. Chem.*, 2004, **76**, 7109.

15 L. Yuan, L. Xu and S. Liu, *Anal. Chem.*, 2012, **84**, 10737.

16 Y. Chi, Y. Dong and G. N. Chen, *Anal. Chem.*, 2007, **79**, 4521.

17 L. J. He, M. S. Wu, J. J. Xu and H. Y. Chen, *Chem. Commun.*, 2013, **49**, 1539.

18 T. Li, Y. Du and E. Wang, *Chem.–Asian J.*, 2008, **3**, 1942.

19 H. Zhu, X. Wang, Y. Li, Z. Wang, F. Yang and X. Yang, *Chem. Commun.*, 2009, 5118.

20 Z. Ding, B. M. Quinn, S. K. Haram, L. E. Pell, B. A. Korgel and A. J. Bard, *Science*, 2002, **296**, 1293.

21 L. Zheng, Y. Chi, Y. Dong, J. Lin and B. Wang, *J. Am. Chem. Soc.*, 2009, **131**, 4564.

22 J. Yu, F. R. F. Fan, S. Pan, V. M. Lynch, K. M. Omer and A. J. Bard, *J. Am. Chem. Soc.*, 2008, **130**, 7196.

23 K. N. Swanick, M. Hesari, M. S. Workentin and Z. Ding, *J. Am. Chem. Soc.*, 2012, **134**, 15205.

24 Y. Chen, Y. Shen, D. Sun, H. Zhang, D. Tian, J. Zhang and J. J. Zhu, *Chem. Commun.*, 2011, **47**, 11733.

25 L. Li, H. Liu, Y. Shen, J. Zhang and J.-J. Zhu, *Anal. Chem.*, 2011, **83**, 661.

26 Y. M. Fang, J. Song, J. Li, Y. W. Wang, H. H. Yang, J. J. Sun and G. N. Chen, *Chem. Commun.*, 2011, **47**, 2369.

27 I. Díez, M. Pusa, S. Kulmala, H. Jiang, A. Walther, A. S. Goldmann, A. H. E. Müller, O. Ikkala and R. H. A. Ras, *Angew. Chem., Int. Ed.*, 2009, **48**, 2122.

28 I. Rubinstein and A. J. Bard, *J. Am. Chem. Soc.*, 1980, **102**, 6641.

29 Z. Guo, Y. Shen, M. Wang, F. Zhao and S. Dong, *Anal. Chem.*, 2003, **76**, 184.

30 J. Li, L. R. Guo, W. Gao, X. H. Xia and L. M. Zheng, *Chem. Commun.*, 2009, 7545.

31 D. Zhu, Y. Tang, D. Xing and W. R. Chen, *Anal. Chem.*, 2008, **80**, 3566.

32 J. H. Zhang, P. Zhan, Z. L. Wang, W. Y. Zhang and N. B. Ming, *J. Mater. Res.*, 2003, **18**, 649.

33 A. Van Blaaderen and A. Vrij, *Langmuir*, 1992, **8**, 2921.

34 L. Wang and E. Wang, *Electrochem. Commun.*, 2004, **6**, 225.

35 L. Jin, L. Shang, S. Guo, Y. Fang, D. Wen, L. Wang, J. Yin and S. k. Dong, *Biosens. Bioelectron.*, 2011, **26**, 1965.